

# Laser $^{40}\text{Ar}/^{39}\text{Ar}$ ages of single detrital white mica grains related to the exhumation of Neoproterozoic and Late Devonian high pressure rocks in the Southern Urals (Russia)

A. P. WILLNER\*, J.-A. WARTHO†, U. KRAMM‡ & V. N. PUCHKOV§

\*Institut für Geologie, Mineralogie und Geophysik, Ruhr-Universität, 44780 Bochum, Germany

†Western Australian Argon Isotope Facility, Department of Applied Geology, Curtin University of Technology, Hayman Road, Bentley WA 6102, Australia

‡Institut für Mineralogie und Lagerstättenlehre, RWTH, Wüllnerstr. 2, 52056 Aachen, Germany

§Ufimian Geoscience Centre, Russian Academy of Science, Karl Marx Street 16/2, 450 000 Ufa, Russia

(Received 20 January 2003; accepted 9 September 2003)

**Abstract** – Single grains of detrital white mica from two different synorogenic sediments in the Southern Urals were analysed using the *in situ* ultraviolet laser ablation Ar–Ar dating technique to discriminate between age signatures associated with a high-pressure signal (phengites) from those related to muscovite only. Two disparately aged sandstone formations of Neoproterozoic (Upper Vendian) and Upper Devonian (Famennian) age were formed by the erosion of high-relief source areas with contemporaneously exhumed high-pressure rocks. A bimodal distribution of ages and chemical compositions can be detected in the two detrital populations. There is no age overlap between the two populations, reflecting completely different source areas containing high-pressure rocks of different ages. Within the Upper Vendian sandstones, detrital white mica from a 571–609 Ma age group is phengitic in composition (Si 3.3–3.41 per formula unit), while an older 645–732 Ma age group is comprised of muscovite composition grains only. The first group is compatible with the time of late exhumation and emplacement of a source area containing high-pressure rocks, the Neoproterozoic Beloretzk terrane. The older age range is compatible with a long history of cooling and the allochthonous nature of this terrane. Detrital white mica from the Famennian sandstones (Zilair Formation) comprises one age group (342–421 Ma) containing phengite (Si 3.21–3.39 per formula unit) and muscovite, and a second group (446–496 Ma) containing muscovite only. While the derivation of the second group cannot be correlated with any as yet known regional data, the first age group indicates the earliest arrival of high-pressure rocks at the surface along the suture zone after Late Devonian arc–continent collision.

Keywords: phengite, detrital minerals, Ar/Ar, laser ablation, Southern Urals, high pressure, Vendian, Famennian.

## 1. Introduction

Synorogenic turbidite sediments can provide evidence of a pre-existing relief, concomitant surface uplift, and the former rock distribution at the surface of their source region. This is particularly important for refining the exhumation history of high-pressure rocks, which is a relatively fast geological process, causing not only considerable disturbance within the crust, but also changes of surface morphology, and an increase in topography. To detect the first appearance of high-pressure rocks at the surface it is necessary to have a detrital component that gives unambiguous evidence of the high-pressure event and allows reasonable geochronological analysis. Phengite (potassic white mica with Si > 3.2 per formula unit) is one possible detrital component, because its composition can retain evidence of elevated pressures of formation in rocks

of the source area (Massonne & Schreyer, 1987; Massonne, 1995). Furthermore, white mica is relatively resistant to erosion and transport processes, is a widespread detrital component, and provides Ar–Ar ages mainly related to formation and/or exhumation of the source rocks (Kelley & Bluck, 1992; Stuart, 2002). On the other hand, muscovite (potassic white mica with Si < 3.2 pfu) can be derived from very different source rocks, high level acid plutons, low-pressure metamorphic rocks, high-pressure rocks without a limiting assemblage, or from retrograde overprints of high-pressure rocks. Considering such a variety of possible source rocks for muscovite relative to phengite, the composition of white micas should be well known before dating. This combination of compositional and age data would enable better resolution of different populations related to disparate source rocks.

In this study we refer to examples from the Southern Urals, where two high-pressure metamorphic complexes of Neoproterozoic and Upper Devonian

\* Author for correspondence: arne.willner@ruhr-uni-bochum.de

ages are the potential (partial) sources for proximal synorogenic turbidite sediments that were deposited in nearby basins during active surface uplift and erosion of these complexes constituting high-relief areas at different times. The scope of this paper is to obtain single grain Ar–Ar ages from detrital white mica grains of known composition, including phengite and muscovite, from these two siliciclastic formations. The resulting age/composition pattern can corroborate and refine previous provenance studies (Willner *et al.* 2001, 2002a, 2003) and yield more detailed information about the surface composition during the already well-known Neoproterozoic and Early Devonian exhumation histories of the two high-pressure metamorphic complexes representing part of the source areas. Furthermore, it is still not known if the Neoproterozoic metamorphic complex also contributed detritus to the Upper Devonian basin. In this case overlapping age/composition signatures in the Neoproterozoic and Upper Devonian sandstone formations would be expected.

## 2. Geological setting and published age data

In the southwestern Urals a 1.8–2.3 Ga old basement is overlain by a 12–15 km thick, mainly siliciclastic Riphean sequence of the extensive Bashkirian basin, where unmetamorphosed Proterozoic sediments were deposited between 1.65 and 0.65 Ga (Maslov *et al.* 1997; Puchkov, 1997). This sedimentation occurred at a stable continental margin of the eastern Baltica protocontinent until around 620 Ma, when a change to active margin conditions occurred during the deposition of Upper Vendian turbidite sandstones, which also involved a change in the derivation of the detritus material (Maslov *et al.* 1997; Willner *et al.* 2001). The Upper Vendian detritus was discharged from a proximal high-relief area in the east and deposited within a foredeep basin on the western flank of a Pre-Uralian orogen (Puchkov, 1997). Detritus composition indicates a ‘recycled orogenic signature’ including mineral and lithic clasts of mainly low-grade siliciclastic metasediments containing phengites with a high pressure signature, as well as clasts of bimodal volcanic rocks and siliciclastic sediments derived from intrabasinal reworking (Willner *et al.* 2001). The absolute age of deposition of the entire Upper Vendian sequence is ~540–620 Ma (Maslov *et al.* 1997; Odin & Odin, 1990). The source area is the Beloretsk Terrane to the east of the Zuratkul Fault, which was deformed by a pre-Uralian Neoproterozoic orogenic event and is characterized by low- to medium-grade metamorphic rocks, the latter dominating in its southern part (Metamorphic Complex of Beloretsk: Glasmacher *et al.* 1999, 2001; Fig. 1). Local lenses of eclogite occur within this complex. The country rocks partly contain phengite, which implies elevated pressure conditions during crystallization. White mica Ar–Ar ages ranging

from  $543 \pm 4$  Ma to  $597 \pm 4$  Ma (Glasmacher *et al.* 1999, 2001) are interpreted as cooling ages and suggest concomitant exhumation, surface uplift, and emplacement of this complex during late Vendian times. However, peak metamorphic conditions must have occurred much earlier as indicated by an Ar–Ar amphibole age of  $718 \pm 5$  Ma (Glasmacher *et al.* 2001). During this time there was ongoing sedimentation within the Riphean basin in the west with sediment input from the west indicating that the Beloretsk Terrane was not yet emplaced and thus presumably had an allochthonous derivation (Glasmacher *et al.* 1999, 2001).

During Early Palaeozoic times, a stable continental margin again developed on the eastern Baltica protocontinent (Puchkov, 1997), until collision with the Magnitogorsk magmatic arc occurred during Late Devonian times. Turbidite sandstones of the Zilair Formation (Famennian to Lower Tournaisian: Pazukhin, Puchkov & Baryshev, 1996 and other references in Willner *et al.* 2002a) were deposited on both sides of an E-dipping suture zone, the Main Uralian Fault (Fig. 1). The detritus is composed of (1) mainly metamorphic lithoclasts and heavy minerals of metamorphic origin (epidote, garnet, tourmaline, Ca-amphibole, glaucophane, chloritoid, titanite and rutile) and to a minor extent by (2) volcanic lithoclasts of a calc-alkaline source, (3) a few serpentinite and chert lithoclasts as well as abundant Cr-spinel from an ophiolitic source, and (4) intraformational sedimentary lithoclasts. The metamorphic source contained low- to medium-grade rocks including high-pressure rocks as indicated by detrital phengite crystals with Si-contents up to 3.45 per formula unit (p.f.u.) and rare detrital glaucophane. Willner *et al.* (2002a) suggested that ophiolites of the Main Uralian Fault zone and metamorphic complexes to the west are the prime source, as well as the volcanosedimentary series of the Magnitogorsk arc. The provenance signature remained unchanged throughout the sedimentation period of the Zilair Formation. This time period (~376–354 Ma, maximum absolute age interval for the Famennian: Tucker *et al.* 1998) represents surface uplift of a narrow ridge or axial rise in the suture zone between the collisional accretionary prism in the west and the forearc basin in the east during exhumation of high-pressure rocks (Willner *et al.* 2002a).

In this potential uplifting source area, two metamorphic complexes were exhumed along the backstop system to the west of the Main Uralian Fault, namely the Suvanyak and Maksyutovo complexes (Fig. 1; Brown *et al.* 1998). The Suvanyak Complex is composed of quartzites, phyllites, and greenschists. So far, nothing is known about the pressure–temperature evolution and exhumation history of these rocks. Brown *et al.* (1998) and Alvarez-Marron *et al.* (2000) interpreted the Suvanyak Complex to represent shallowly subducted continental shelf and rise material.

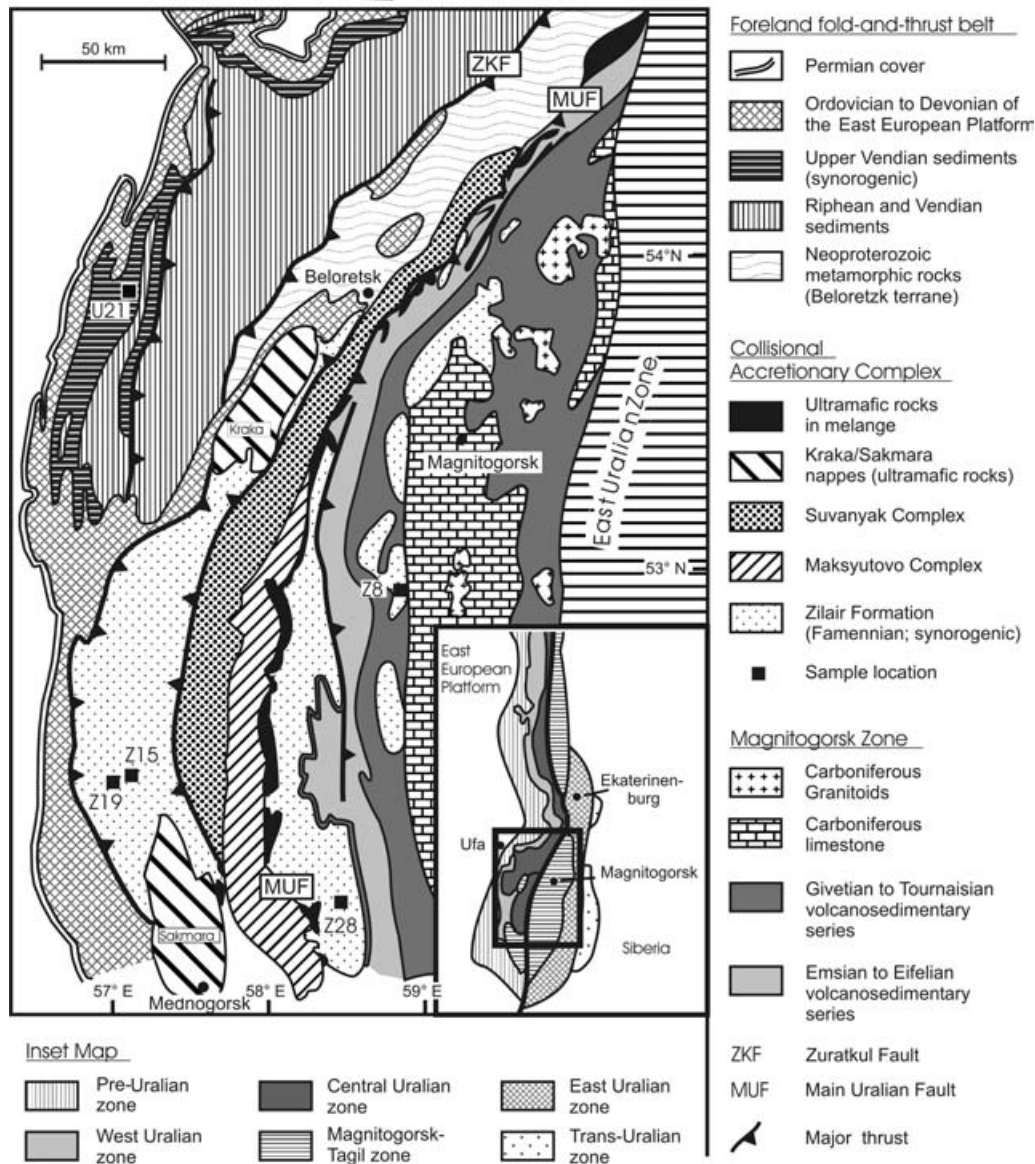


Figure 1. Geological map of the southwestern Urals (modified after Brown *et al.* 1998, 2001).

The Maksyutovo Complex is composed of medium-grade, high-pressure rocks thought to represent thinned continental crust of the East European continental margin that was subducted during the Late Devonian continent/arc collision (Hetzl, 1999). The Maksyutovo Complex is subdivided into two major units (1 and 2). A heterogeneous, structurally lower Unit 1 is mainly composed of metagreywackes, quartzites and garnet-mica schists with lenses of graphitic schists, eclogites, jadeite-quartzite blocks, and blueschists. Peak metamorphic conditions ranged from 15 to 23 kbar and 550–650 °C (Beane *et al.* 1995; Schulte & Blümel, 1999). The isotopic ages of the high-pressure rocks of Unit 1 range from 382 ± 10 Ma to 357 ± 15 Ma (Sm–Nd mineral isochrons: Shatsky, Jagoutz & Koz’menko, 1997; Beane & Connelly, 2000), 384 ± 3 Ma to 377 ± 2 Ma (U/Pb, rutile: Beane & Connelly, 2000) and 388 ± 4 Ma to 356 Ma ± 2 Ma (Ar–Ar,

white mica: Matte *et al.* 1993; Lennykh *et al.* 1995; Beane & Connelly, 2000) and are interpreted to date the early exhumation and cooling after peak metamorphic conditions. The narrow range of the ages derived from different minerals and geochronological techniques with differing closure temperatures suggest initial exhumation rates of > 1.5 mm a<sup>-1</sup> within a time interval that roughly coincides with the absolute age of deposition of the Zilair Formation (~ 376–354 Ma; see above). Recent high-precision Rb/Sr mineral isochron data on eclogites (Glodny *et al.* 2002) could confine the age of high-pressure metamorphism to 375 ± 2 Ma in several localities. Determining Rb–Sr white mica ages in exhumation-related mylonites, Hetzel & Romer (2000) suggested that the Maksyutovo Complex reached mid-crustal levels at 360 ± 8 Ma resulting in an early relatively moderate mean exhumation rate of ~ 2–3 mm a<sup>-1</sup> compared to collisional high-pressure rocks

worldwide. On the other hand, considerable changes in arc/forearc tectonics within the Magnitogorsk arc during the Givetian (absolute age range of  $\sim 387$ – $382$  Ma; Tucker *et al.* 1998) suggest the full arrival of European continental crust in the subduction zone at that time (Brown *et al.* 2001).

The structurally overlying Unit 2 of the Maksyutovo Complex mainly contains lower-grade stilpnomelane quartzite and phyllite, eclogite, greenschist, marble, lawsonite-bearing rocks, and lenses of serpentinite. Peak metamorphic conditions in this unit are considered to be around  $450^\circ\text{C}$ , 8 kbar (Hetzl *et al.* 1998), with rodingitized ultramafic blocks within a basal shear zone retaining peak metamorphic conditions of  $520$ – $540^\circ\text{C}$ , 18–21 kbar (Schulte & Sindern, 2002). Ar–Ar white mica ages from the Unit 2 range from  $339 \pm 2$  to  $332 \pm 4$  Ma (Beane & Connelly, 2000), and Rb–Sr formation ages for white micas, overprinting the ultramafic blocks at its base, are  $339 \pm 6$  and  $338 \pm 5$  Ma (Schulte & Sindern, 2002). Units 1 and 2 were emplaced against each other along a major retrograde shear zone with normal fault kinematics under greenschist facies conditions (Hetzl, 1999). It becomes apparent that the exposed Unit 1 cannot be the direct source of the Zilair Formation, because it was at a mid-crustal level, when sedimentation of the Zilair Formation had ceased.

Apatite fission track ages indicate closing at a temperature of  $110^\circ\text{C}$  by  $\sim 315$  Ma suggesting a mean exhumation rate of  $\sim 0.3$  mm  $\text{a}^{-1}$  from the middle to the upper crust followed by minor reheating and slower cooling and exhumation of  $< 0.1$  mm  $\text{a}^{-1}$  between 315 Ma and 230 Ma due to tectonic reburial (Leech & Stockli, 2000). This is consistent with the slowing down of convergence and surface uplift, termination of magmatic activity in the arc, peneplanization and development of a carbonate platform next to the suture zone during Early Carboniferous times (Puchkov, 1997). A second phase of Uralian collision occurred during the Late Carboniferous/Early Permian after a major temporal break, when collisional processes took place within the East Uralian zone. During this later convergence, the former margin was deformed into a W-verging fold-and-thrust belt (Brown *et al.* 1997; Giese *et al.* 1999). This deformation was accompanied by a new phase of erosion and a much slower exhumation of the metamorphic rocks. The erosion came almost to an end by the Late Permian when the Tethyan seas penetrated the East- and Trans-Uralian zones, but it was resumed again in the Triassic until the Devonian Maksyutovo metamorphic rocks were finally overlain by thin Cretaceous marine sediments (Puchkov, 2000).

### 3. Analytical methods

One sandstone sample (U21) from the Zigan Formation in the uppermost part of the Upper Vendian succession

and four sandstone samples from the Zilair Formation (Z8, Z15, Z19 and Z28; Fig. 1; see Willner *et al.* 2001 for petrography) were selected. Sample localities are listed in the Appendix. Samples Z15 and Z19 are from the Middle Zilair Formation, west of the Main Uralian Fault, and samples Z8 and Z28 are from the Lower Zilair Formation to the east of the Main Uralian Fault (Fig. 1; see Willner *et al.* 2002b for petrography). In both formations the detrital white mica populations contain muscovite and phengite (Willner *et al.* 2001, 2002a). As both chemical composition and geochronological information needed to be obtained from the individual grains, electron microprobe analysis and *in situ* ultraviolet laser ablation dating were applied to the same grains. Ar–Ar dating of detrital grains is more usually undertaken on crushed and separated individual grains, using infra-red or visible lasers to totally fuse each grain. Unless the grains are both large and old, it is generally not possible to undertake laser step-heating on individual detrital grains. Two polished sections of  $10\text{ mm} \times 10\text{ mm} \times 150\ \mu\text{m}$  were prepared for each sample. The individual white mica clasts were selected, photographed and analysed using a CAMECA SX 50 electron microprobe at Bochum University (for analytical details see Willner *et al.* 2001). All sections analysed were cut perpendicular to (001) of the white mica clasts (see Table 1 for individual grain sizes).

The Ar–Ar data presented in this study were obtained at the Western Australian Argon Isotope Facility in Perth, operated by a consortium consisting of Curtin University and the University of Western Australia. At Curtin University, the polished thick sections were removed from their glass slides and underwent ultrasonic treatment in methanol and subsequently deionized water. Samples were individually wrapped in aluminium foil and all the samples were loaded into an aluminium package. Biotite age standard Tinto B, with a K–Ar age of  $409.24 \pm 0.71$  Ma, was loaded at 5 mm intervals along the Al irradiation package to monitor the neutron flux gradient. The package was Cd-shielded and irradiated with fast neutrons in the H5 position of the McMaster University Nuclear Reactor, Hamilton, Canada, for 20 hours. Upon return to Curtin University, the samples were loaded into an ultra-high vacuum laser chamber with a Suprasil 2 window and baked to  $120^\circ\text{C}$  overnight to remove adsorbed atmospheric argon from the samples and chamber walls.

A New Wave Research LUV 213X 4 mJ pulsed quintupled Nd-YAG laser ( $\lambda = 213$  nm), with a variable spot size of  $10$ – $350\ \mu\text{m}$ , and a repetition rate of 10 Hz, was used to ablate the individual mineral grains. The laser was fired through a Merchanteck computer-controlled X–Y–Z sample chamber stage and microscope system, fitted with a high-resolution CCD camera,  $6\times$  computer controlled zoom, high magnification objective lens, and two light sources for sample illumination. A rim of  $2$ – $5\ \mu\text{m}$  was left during

Table 1. Measured isotopic ratios and Ar–Ar ages for detrital white micas (errors are  $1\sigma$ )

Sample	Grain	Size <sup>1</sup>	Age (Ma)	±	<sup>40</sup> Ar*/ <sup>39</sup> Ar	±	<sup>40</sup> Ar/ <sup>39</sup> Ar	±	<sup>38</sup> Ar/ <sup>39</sup> Ar	±	<sup>37</sup> Ar/ <sup>39</sup> Ar	±	<sup>36</sup> Ar/ <sup>39</sup> Ar	±	<sup>39</sup> Ar (cm <sup>3</sup> )	Ar	±
Zigan Formation Upper Vendian																	
U21	P18	200/67	242.15	31.70	31.27	4.37	94.75	1.98	0.06329	0.00594	2.65354	0.11071	0.21484	0.01330	6.85E-13	67.00	4.66
U21	P83 <sup>2</sup>	91/55	571.04	26.18	81.05	4.32	95.84	3.78	0.02468	0.00479	0.54455	0.11755	0.05006	0.00718	5.67E-13	15.43	5.61
U21	P57 <sup>2</sup>	n.d.	585.52	16.17	83.46	2.67	98.29	1.62	0.01850	0.00358	0.00000	0.00000	0.05018	0.00717	3.78E-13	15.09	3.05
U21	P48 <sup>2</sup>	68/31	594.14	20.59	84.90	3.43	98.19	2.21	0.03251	0.00451	0.06133	0.04498	0.04496	0.00900	3.01E-13	13.53	4.00
U21	P84 <sup>2</sup>	n.d.	609.22	2.61	87.44	0.05	96.13	0.05	0.02431	0.00000	0.02686	0.02643	0.02942	0.00000	4.60E-13	9.04	0.07
U21	P53	140/57	645.00	41.13	93.55	7.08	103.94	6.19	0.01621	0.00785	0.64845	0.19295	0.03516	0.01178	3.45E-13	10.00	8.67
U21	P74	96/54	655.15	20.18	95.31	3.47	102.20	2.60	0.01878	0.00779	0.23273	0.04582	0.02332	0.00780	5.22E-13	6.74	4.14
U21	P61	120/63	658.13	21.53	95.82	3.71	99.30	3.10	0.03665	0.00713	0.21153	0.04672	0.01178	0.00710	5.73E-13	3.50	4.80
U21	P85	163/57	680.71	10.80	99.77	1.83	102.63	1.36	0.01003	0.00416	0.14929	0.02448	0.00968	0.00416	9.76E-13	2.79	2.20
U21	P27	66/54	708.51	32.46	104.70	5.78	111.04	4.34	0.03119	0.01295	0.46366	0.07617	0.02146	0.01295	3.14E-13	5.71	6.38
U21	P86	n.d.	732.41	4.52	109.00	0.61	135.21	0.75	0.03434	0.00019	0.00000	0.00000	0.08868	0.00049	4.89E-13	19.38	0.64
Zilair Formation (Famennian)																	
Z8	P6a	171/27	250.41	52.18	32.47	7.25	55.67	1.16	0.00938	0.00303	0.95123	0.03101	0.07850	0.02423	4.47E-13	41.67	13.07
Z8	P2a <sup>2</sup>	132/16	318.49	122.59	42.11	17.68	68.30	2.73	0.03816	0.00740	0.23567	0.07409	0.08864	0.05913	1.83E-13	38.35	26.00
Z8	P8a <sup>2</sup>	443/107	380.45	52.90	51.20	7.89	58.97	1.21	0.01022	0.00330	0.43622	0.03313	0.02629	0.02640	4.11E-13	13.17	13.50
Z15	P2b <sup>2</sup>	150/28	311.86	55.47	41.09	7.96	55.18	3.61	0.03718	0.00022	1.33807	0.42139	0.04767	0.02401	2.26E-13	25.53	15.22
Z15	P12b <sup>2</sup>	115/23	313.03	23.82	41.26	3.41	49.80	1.87	0.01500	0.00484	0.53869	0.17670	0.02891	0.00968	2.80E-13	17.15	7.52
Z15	P3b <sup>2</sup>	259/61	385.84	11.60	51.93	1.71	52.91	1.39	0.02103	0.00679	0.34788	0.03114	0.00330	0.00339	3.99E-13	1.85	4.14
Z15	P4a	257/53	446.20	53.52	61.11	8.27	64.78	3.76	0.00000	0.00000	0.05553	0.43714	0.01245	0.02493	2.17E-13	5.68	13.88
Z19	P8a	123/46	332.97	23.31	44.19	3.38	49.70	1.94	0.00485	0.00470	0.52306	0.17164	0.01866	0.00940	2.88E-13	11.09	7.64
Z19	P28a	141/27	342.32	21.36	45.55	3.11	48.55	0.72	0.00794	0.00256	0.45225	0.05247	0.01014	0.01025	5.29E-13	6.17	6.56
Z19	P17b	127/30	325.04	1.57	43.04	0.07	66.34	0.07	0.03701	0.00000	0.00000	0.00000	0.07885	0.00000	3.78E-13	35.12	0.13
Z19	P14b	153/18	496.19	2.40	69.02	0.16	69.02	0.16	0.00000	0.00000	1.01746	0.00000	0.00000	0.00000	1.68E-13	0.00	0.33
Z19	P6b	248/28	409.59	2.08	55.56	0.15	58.84	0.15	0.00000	0.00000	0.54330	0.05346	0.01108	0.00000	2.42E-13	5.57	0.34
Z28	P3a	128/18	339.36	21.67	45.09	3.15	60.04	1.26	0.00000	0.00000	0.57569	0.09513	0.05058	0.01020	1.34E-13	24.90	5.48
Z28	P2a	180/85	402.04	7.44	54.39	1.09	57.26	0.53	0.02023	0.00019	0.21608	0.04300	0.00974	0.00327	4.15E-13	5.03	2.10
Z28	P1a	174/20	468.18	27.61	64.55	4.31	77.17	1.12	0.02939	0.00042	0.00000	0.00000	0.04269	0.01424	1.90E-13	16.35	5.72
Z28	P5b	97/28	382.60	43.13	51.47	6.43	64.98	1.92	0.02580	0.00024	0.34859	0.15248	0.04572	0.02082	3.25E-13	20.79	10.18
Z28	P3b	117/48	388.91	36.34	52.41	5.44	57.59	1.61	0.02907	0.00023	0.29445	0.12879	0.01752	0.01759	3.85E-13	8.99	9.78
Z28	P2b	165/27	421.64	12.63	57.36	1.91	57.35	1.55	0.00000	0.00000	0.07016	0.03452	0.00000	0.00000	3.60E-13	0.00	4.28

1 – Mean length parallel trace of (001)/mean width perpendicular trace of (001) (in  $\mu\text{m}$ ); n.d. – not documented; 2 – phengite J values used for the samples are U21 –  $0.004594 \pm 0.000023$ , Z8 –  $0.004585 \pm 0.000023$ , Z15 –  $0.004592 \pm 0.000023$ , Z19 –  $0.004587 \pm 0.000023$ , Z28 –  $0.004590 \pm 0.000023$ .

ablation of an individual grain to avoid contamination with neighbouring phases.

The gases released by laser ablation analysis were 'gettered' using 3 SAES AP10 getter pumps to remove all active gases. The remaining noble gases were equilibrated into a high sensitivity MAP 215-50 mass spectrometer, operated at a resolution of 600, and fitted with a Balzers SEV 217 multiplier. The automated extraction and data acquisition system was computer controlled, using a LabView program. The mean five-minute extraction system blank Ar isotope measurements obtained during the experiments were  $8.9 \times 10^{-12}$ ,  $5.4 \times 10^{-15}$ ,  $8.1 \times 10^{-15}$ ,  $1.2 \times 10^{-13}$ , and  $4.9 \times 10^{-14}$  cm<sup>3</sup> STP (standard temperature and pressure) for <sup>40</sup>Ar, <sup>39</sup>Ar, <sup>38</sup>Ar, <sup>37</sup>Ar and <sup>36</sup>Ar respectively. Samples were corrected for mass spectrometer discrimination and nuclear interference reactions (<sup>39</sup>Ar/<sup>37</sup>Ar<sub>Ca</sub> = 0.00065, <sup>36</sup>Ar/<sup>37</sup>Ar<sub>Ca</sub> = 0.000255 and <sup>40</sup>Ar/<sup>39</sup>Ar<sub>K</sub> = 0.0015). Errors quoted on the ages are at a 1σ level, and Ar–Ar ages were calculated using the decay constant quoted by Steiger & Jäger (1977). The J values and errors are noted in Table 1.

#### 4. Geochronological results

The white mica populations from both sandstone formations show different age distributions with no overlap (Table 1, Figs 2, 3). In both white mica populations a few grains with ages younger than the presumed age of sedimentation were obtained (Table 1). One grain (U21-P18) from Upper Vendian Zigan Formation, and three grains from the Famennian Zilair Formation samples (Z8-P6a, Z15-P12b and Z19-P17b) yielded Ar–Ar ages much younger and not within error of the absolute deposition ages of the sedimentary sequences, 540–620 Ma (Upper Vendian) and 354–376 Ma (Famennian), respectively (see Section 2). Furthermore, five other Famennian white mica grains yielded young ages; however, because the individual errors were large for these analyses, they fall within error of the deposition age range of 354–376 Ma (Table 1). Most of the Ar–Ar analyses of these detrital white mica grains have large associated errors, which is mainly due to the very small quantities of <sup>40</sup>Ar recovered during *in situ* ultraviolet laser ablation. <sup>40</sup>Ar values were generally only two to six times higher than blank levels. In the following, we will first discuss effects leading to the exceptionally young ages to exclude their influence on the remaining data.

One possible cause of young ages may be due to post-depositional heating resulting in some radiogenic <sup>40</sup>Ar (<sup>40</sup>Ar\*) loss and resetting of the Ar–Ar ages. Matenaar *et al.* (1999) reported illite crystallinity values within the Zilair Formation from anchizonal up to epizonal in the Zilair syncline, west of the Main Uralian Fault. This can be attributed to late stacking of the foreland belt after 315 Ma. There are no available illite crystallinity data from our study areas, but temperatures in excess

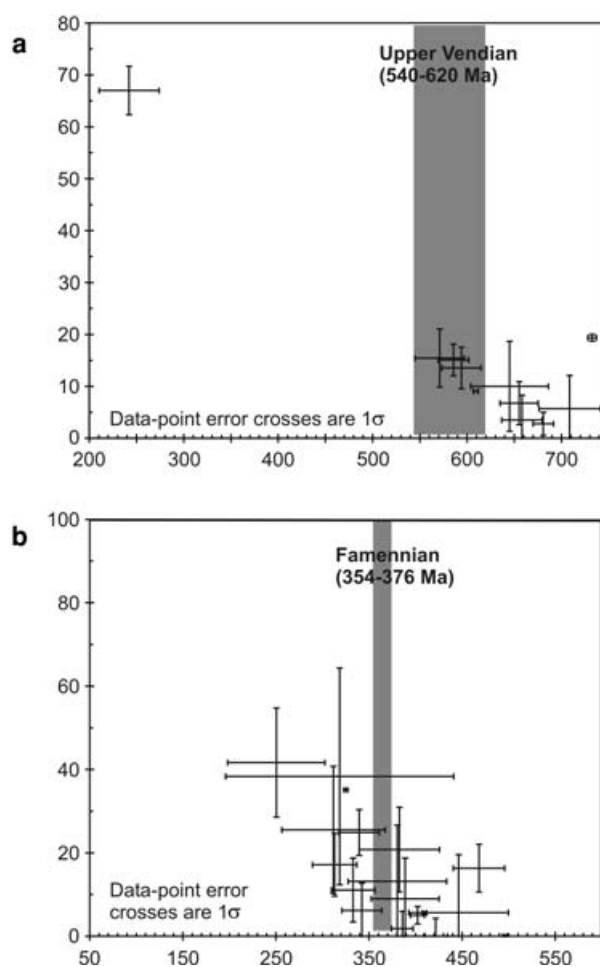


Figure 2. Plot of the percentage of atmospheric Ar v. Ar–Ar age for (a) detrital white micas from the Upper Vendian Zigan Formation and (b) detrital white micas from the Famennian Zilair Formation. Shaded strips indicate the approximate time of deposition of the respective sequences.

of 300°C can be excluded owing to a lack of any quartz recrystallization in the matrix of the sandstones. Assuming maximum temperatures of 250°C for a duration of 50 Ma, we calculated the potential <sup>40</sup>Ar\* loss, for both the minimum and maximum grain diameters, using the Ar diffusion parameters of Hames & Bowring (1994). The potential loss of 1.1–5.7% <sup>40</sup>Ar\* would result in an age reduction of 3.8 to 20.7 Ma for the Devonian white micas. For the Upper Vendian sandstones, which have only been subjected to diagenetic conditions after deposition, the effect of potential age resetting is negligible (<0.4% <sup>40</sup>Ar\* loss). There is no direct correlation between grain size and age, and the calculated maximum potential reduction of age by possible reheating cannot explain the observed very young ages.

The grains with ages younger than the sedimentation age all have high concentrations of atmospheric Ar (<sup>36</sup>Ar) in both Upper Vendian and Upper Devonian populations. There is a clear negative correlation

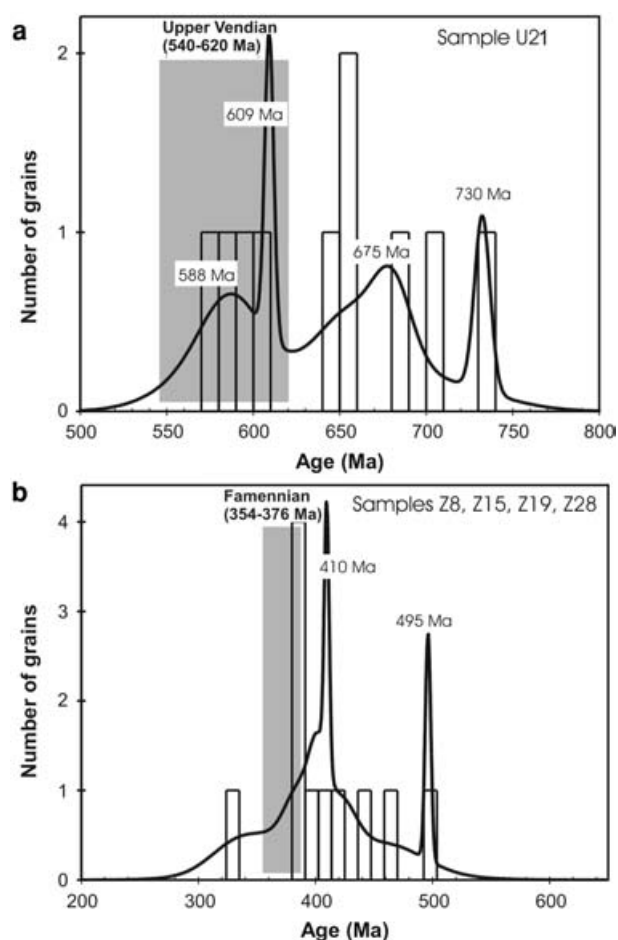


Figure 3. Distribution of ages including a probability curve for (a) detrital white micas from the Upper Vendian Zigan Formation and (b) detrital white mica from the Famennian Zilair Formation. Shaded strips indicate the approximate time of deposition of the respective sequences.

between the calculated percentage of atmospheric Ar in the dated grains and their apparent Ar–Ar ages (Fig. 2), suggesting the possibility of low temperature alteration in these grains. In a similar study of single grain Ar–Ar ages from detrital muscovites in recent sands of the Bengal Fan, Copeland & Harrison (1990) found two grains that showed significantly younger ages than their stratigraphic age and anomalously high  $^{36}\text{Ar}$  contents, and they attributed this to possible contamination by hydrocarbons interfering with the  $^{36}\text{Ar}$  peak. However, hydrocarbons are not considered to be the cause of the high atmospheric Ar contents for the young grains analysed in our study, because the presence of hydrocarbons is routinely checked during analyses of mass 41 (that is,  $\text{C}_3\text{H}_5$ , a by-product of hydrocarbon cracking during ionization at the mass spectrometer source) and no anomalously high concentrations were detected for any of the grains.

Another process that can introduce atmospheric Ar is ‘seritization’ of white mica grains. Although Clauer

(1981) showed that Ar–Ar ages of white micas were not reset by intense *in situ* weathering, McDowell & Elders (1980) reported alteration of muscovite to illite in the Salton Sea System at temperatures  $\leq 280^\circ\text{C}$ . The introduction of atmospheric Ar during an exogenetic process prior to sedimentation may have resulted in removal of  $^{40}\text{Ar}^*$ , thus causing an apparent younging of ages. Considerable loss of K and  $^{40}\text{Ar}^*$  as the cause of young ages can be excluded on the basis of the electron microprobe analyses; there was normal occupation of the interlayer sites (Table 2).

‘Illitization’ of white micas along cleavage planes, resulting in the loss of diffusion length scale leading to enhanced  $^{40}\text{Ar}^*$  loss during a later reheating event, and a heterogeneous mix of phases can also yield  $^{39}\text{Ar}$  recoil problems. During neutron irradiation, fine-grained or finely interlayered phases can suffer from  $^{39}\text{Ar}$  redistribution and loss via recoil, due to the interaction of the different mineral phases with fast neutrons. From Ar–Ar step-heating studies on multi-grain samples, this has been shown to result in either young or old geologically meaningless ages (Hess & Lippolt, 1986; Lo & Onstott, 1989).

Cumulative probability or Gaussian plots, with histograms, of the two sets of samples are plotted to show the age distribution of detrital grains from geochronological studies (Fig. 3), which sum the Gaussian error distribution curves for the individual grains. Excluding the one anomalously young grain (U21-P18), the age distribution of the Upper Vendian detrital white micas yielded four modes. The youngest two modes are found at approximately 588 and 609 Ma. These two modes correspond to the 571–609 Ma age range of four white mica grains of phengitic composition (Si 3.3–3.41 p.f.u.; Table 2). The two older modes with Ar–Ar ages around 675 Ma and 730 Ma contain six grains with an age range of 645–732 Ma and muscovite compositions (Si 3.0–3.06 p.f.u.; Table 2). The Ti-contents of the second set (0.034–0.082 p.f.u.) are significantly different from those of the first set (0.003–0.033 p.f.u.). Otherwise, the mineral chemistry is fairly variable as might be expected for detrital micas.

Excluding seven grains that yielded anomalously young ages and high atmospheric Ar contents ( $> c. 20\%$ ), the age distribution of the remaining eleven Devonian Zilair Formation white micas yielded age modes of approximately 410 Ma and 495 Ma. The 410 Ma group, with an age range of 342–421 Ma, contains four phengite grains (Si 3.21–3.39 p.f.u.) and four muscovite grains (Si 3.01–3.15 p.f.u.), while the three grains that yielded the older 495 Ma ages (446–496 Ma) contained muscovite compositions only (Si 3.0–3.02 p.f.u.). Therefore, similar to the distribution type of the Upper Vendian detrital white mica population, a bimodal distribution of ages and mineral composition is also apparent in the Upper Devonian detrital white micas.

Table 2. Microprobe analyses of dated white mica grains

	Zigan Formation (Upper Vendian)												Zilair Formation (Famennian)																
	U21												Z19					Z28					Z15				Z8		
	P18	P27	P48	P53	P57	P61	P74	P83	P84	P85	P86		P28a	P6b	P8b	P14b	P17b	P1a	P2a	P3a	P2b	P3b	P5b	P4a	P2b	P3b	P12b	P2a	P6a
SiO <sub>2</sub>	44.25	44.87	48.47	44.81	50.04	44.49	44.03	49.45	47.76	43.96	43.82	44.73	46.54	45.11	45.15	44.07	45.45	48.94	47.13	47.67	44.69	44.67	45.09	47.59	49.60	48.92	45.05	45.84	48.07
TiO <sub>2</sub>	0.81	0.33	0.32	0.71	0.03	0.52	0.34	0.20	0.14	0.66	0.60	0.04	0.31	0.23	0.13	0.48	0.20	0.07	0.51	0.01	0.24	0.87	0.77	0.19	0.07	0.18	1.00	1.52	0.06
Al <sub>2</sub> O <sub>3</sub>	35.81	32.86	28.28	35.08	26.15	36.14	35.36	26.54	24.19	30.82	34.62	34.11	31.52	34.68	36.77	34.91	36.94	25.14	33.53	31.45	36.20	35.93	35.89	32.43	28.84	27.68	35.83	28.14	30.02
FeO	1.48	3.33	4.23	1.87	3.15	1.15	1.56	4.75	7.37	6.05	3.02	2.70	4.51	3.09	1.25	3.06	1.41	5.01	2.25	2.98	1.41	1.09	1.36	2.67	2.65	5.04	1.42	5.47	2.87
MnO	0.00	0.02	0.03	0.01	0.06	0.00	1.56	0.00	0.00	0.09	0.00	0.14	0.04	0.05	0.03	0.00	0.00	0.08	0.01	0.03	0.05	0.04	0.00	0.01	0.00	0.02	0.00	0.12	0.00
MgO	0.54	1.44	2.24	0.83	3.27	0.52	0.78	2.89	2.72	1.34	0.59	1.54	1.40	0.57	0.48	0.56	0.55	3.11	1.64	2.11	0.48	0.52	0.62	1.59	2.95	2.72	0.63	3.04	2.25
CaO	0.05	0.06	0.12	0.02	0.12	0.41	0.05	0.05	0.04	0.00	0.07	0.14	0.20	0.00	0.02	0.05	0.02	0.09	0.10	0.12	0.04	0.00	0.03	0.04	0.00	0.07	0.12	1.50	0.08
BaO	0.30	1.16	0.19	0.18	0.20	0.46	0.22	0.11	0.18	0.29	0.29	0.09	0.11	0.30	0.32	0.37	0.39	0.46	0.40	0.15	0.28	0.28	0.48	0.39	0.40	0.19	0.20	0.23	0.37
Na <sub>2</sub> O	1.15	0.31	0.63	0.52	0.11	0.80	0.68	0.11	0.10	0.32	1.03	0.39	1.52	1.27	1.67	0.71	1.00	0.20	0.67	0.95	0.87	1.07	0.98	0.53	0.17	0.48	0.98	0.09	0.10
K <sub>2</sub> O	10.00	10.50	9.73	10.47	10.96	9.98	10.54	10.33	10.98	10.82	10.07	10.51	8.56	9.17	8.91	10.43	9.90	10.80	9.05	8.97	10.06	9.47	9.81	10.21	10.24	10.54	8.98	9.26	10.87
Cl	0.01	0.03	0.00	0.04	0.01	0.02	0.02	0.00	0.03	0.02	0.02	0.01	0.00	0.01	0.05	0.02	0.02	0.00	0.00	0.00	0.00	0.05	0.02	0.01	0.00	0.00	0.02	0.02	0.01
F	0.00	0.00	0.00	0.00	0.04	0.00	0.00	0.04	0.10	0.00	0.03	0.00	0.04	0.02	0.08	0.00	0.00	0.00	0.02	0.00	0.03	0.00	0.00	0.02	0.14	0.12	0.00	0.00	0.06
H <sub>2</sub> O*	4.43	4.37	4.40	4.43	4.37	4.44	4.42	4.37	4.21	4.30	4.36	4.41	4.41	4.42	4.44	4.40	4.52	4.32	4.50	4.45	4.43	4.43	4.47	4.47	4.40	4.38	4.46	4.37	4.39
Total**	98.83	99.28	98.64	99.04	98.51	98.93	99.56	98.84	97.62	98.66	98.50	98.81	99.14	98.91	99.26	99.06	100.40	98.22	99.80	98.89	98.77	98.41	99.52	100.14	99.40	100.29	98.69	99.60	99.12
Si	5.983	6.140	6.611	6.055	6.830	5.999	5.966	6.750	6.715	6.128	5.998	6.083	6.308	6.105	6.031	6.004	6.026	6.787	6.273	6.418	6.029	6.028	6.040	6.361	6.665	6.618	6.046	6.280	6.517
Alt	2.017	1.860	1.389	1.946	1.170	1.269	2.034	1.250	1.285	1.872	2.002	1.917	1.692	1.895	1.969	1.996	1.974	1.214	1.727	1.582	1.971	1.973	1.960	1.639	1.335	1.383	1.954	1.720	1.483
Total	8.000	8.000	8.000	8.000	8.000	8.000	8.000	8.000	8.000	8.000	8.000	8.000	8.000	8.000	8.000	8.000	8.000	8.000	8.000	8.000	8.000	8.000	8.000	8.000	8.000	8.000	8.000	8.000	8.000
Alo	3.690	3.440	3.156	3.642	3.036	3.744	3.613	3.020	2.775	3.191	3.583	3.550	3.343	3.638	3.819	3.610	3.798	2.895	3.533	3.408	3.786	3.741	3.706	3.469	3.232	3.030	3.713	2.824	3.313
Ti	0.082	0.034	0.033	0.072	0.003	0.054	0.035	0.021	0.013	0.069	0.062	0.004	0.032	0.023	0.013	0.049	0.020	0.007	0.051	0.001	0.024	0.088	0.078	0.019	0.007	0.018	0.101	0.157	0.006
Fe	0.167	0.381	0.482	0.212	0.360	0.130	0.177	0.542	0.867	0.705	0.346	0.307	0.511	0.350	0.140	0.349	0.156	0.581	0.250	0.336	0.159	0.123	0.152	0.298	0.298	0.570	0.159	0.627	0.325
Mn	0.000	0.002	0.004	0.001	0.007	0.000	0.179	0.000	0.000	0.011	0.000	0.016	0.005	0.005	0.003	0.000	0.000	0.009	0.001	0.003	0.006	0.005	0.000	0.001	0.000	0.002	0.000	0.014	0.000
Mg	0.109	0.294	0.455	0.167	0.665	0.105	0.158	0.588	0.570	0.278	0.120	0.313	0.283	0.115	0.096	0.114	0.109	0.643	0.325	0.423	0.097	0.105	0.124	0.317	0.591	0.548	0.126	0.621	0.455
Total	4.049	4.151	4.130	4.094	4.071	4.033	4.161	4.171	4.225	4.255	4.111	4.190	4.173	4.131	4.071	4.121	4.083	4.136	4.160	4.171	4.072	4.062	4.059	4.105	4.128	4.169	4.100	4.242	4.099
Ca	0.007	0.009	0.018	0.003	0.018	0.059	0.007	0.007	0.006	0.000	0.010	0.021	0.029	0.000	0.003	0.007	0.003	0.013	0.014	0.017	0.005	0.000	0.004	0.006	0.000	0.010	0.017	0.220	0.012
Ba	0.016	0.062	0.010	0.010	0.011	0.025	0.012	0.006	0.010	0.016	0.016	0.005	0.006	0.016	0.017	0.020	0.020	0.025	0.021	0.008	0.015	0.015	0.025	0.020	0.021	0.010	0.011	0.012	0.020
Na	0.302	0.082	0.167	0.136	0.029	0.210	0.179	0.029	0.028	0.087	0.273	0.103	0.399	0.334	0.433	0.188	0.257	0.054	0.173	0.248	0.226	0.280	0.255	0.137	0.044	0.126	0.255	0.024	0.026
K	1.725	1.833	1.693	1.805	1.908	1.716	1.822	1.799	1.969	1.924	1.758	1.823	1.480	1.583	1.518	1.813	1.674	1.910	1.536	1.540	1.732	1.630	1.676	1.741	1.755	1.819	1.537	1.618	1.880
Total	2.049	1.986	1.887	1.953	1.966	2.010	2.020	1.841	2.013	2.026	2.058	1.952	1.914	1.933	1.970	2.027	1.954	2.003	1.744	1.814	1.978	1.925	1.960	1.904	1.820	1.965	1.820	1.875	1.937
Cl	0.002	0.007	0.000	0.008	0.002	0.004	0.005	0.000	0.007	0.005	0.005	0.001	0.000	0.002	0.011	0.005	0.005	0.000	0.000	0.000	0.000	0.011	0.005	0.002	0.000	0.000	0.005	0.005	0.002
F	0.000	0.000	0.000	0.001	0.017	0.000	0.000	0.017	0.046	0.000	0.013	0.000	0.017	0.009	0.034	0.000	0.000	0.000	0.008	0.000	0.011	0.000	0.000	0.009	0.060	0.051	0.000	0.000	0.026
OH	3.998	3.993	4.000	3.991	3.980	3.996	3.995	3.983	3.947	3.995	3.982	3.999	3.983	3.988	3.955	3.995	3.996	4.000	3.992	4.000	3.989	3.989	3.996	3.989	3.941	3.949	3.996	3.995	3.972

\* – calculated; \*\* – Total corrected for F and Cl; cations calculated on the basis of 44 negative valencies; Alo – Al in octahedral position; Alt – Al in tetrahedral position.



## 5. Discussion and regional constraints

The Neoproterozoic phengitic white mica population with an Ar–Ar age range of 571–609 Ma from sample U21 of the Zigan Formation agrees with the white mica age range of 543–597 Ma from the Beloretzk Complex (Glasmacher *et al.* 1999, 2001), which formed part of the potential source region. Furthermore, the age range falls within the time of deposition of the Upper Vendian synorogenic sediments (~540–620 Ma) indicating contemporaneous exhumation, cooling, uplift, erosion and sedimentation. The  $571.0 \pm 26.2$  Ma Ar–Ar age from detrital grain U21-P83 provides an approximate indicator of the maximum age of the Upper Vendian Zigan Formation. The fact that there are no white micas older than 732 Ma suggests no contribution from the basement of the East European platform or from recycled Riphean sediments. For the muscovites with Ar–Ar ages ranging from 645 to 732 Ma, a magmatic source cannot be excluded. Although white mica-bearing granites seem to be very rare in the exposed potential source region, and there are relatively few hints of plutonic source rocks in the Upper Vendian detritus (Willner *et al.* 2001), some pebbles of two-mica granites occur in the Upper Vendian Kukkarauk conglomerate immediately below the Zigan Formation. Glasmacher *et al.* (2001) obtained a muscovite Ar–Ar plateau age of  $699 \pm 3$  Ma from such a granite pebble. The slightly enhanced Ti-contents of the muscovites could also be due to a higher temperature of formation. On the other hand, many grains of the muscovite population may be derived from metamorphic sequences. Glasmacher *et al.* (1999, 2001) considered a long period of cooling and exhumation of the Beloretzk Complex based on amphibole Ar–Ar cooling ages around  $718 \pm 5$  Ma. Two muscovite samples from the southwestern part of the Beloretzk Complex yielded Ar–Ar age spectra with age gradients of 575–615 Ma and 575–680 Ma (Glasmacher *et al.* 2001). Our data would further support this slow cooling and exhumation hypothesis, because the range of Ar–Ar ages obtained from the detrital white micas matches this long interval. Whatever process formed the muscovites found within the Upper Vendian sandstones, no processes of a corresponding age forming or altering white micas are known from the Riphean basin to the west, where sedimentation continued at that time. This further corroborates the allochthonous nature of the supposed source area proposed by Glasmacher *et al.* (1999, 2001).

No overlapping ages were found between the Upper Vendian and Upper Devonian detrital white mica populations, indicating that the Upper Devonian Zilair Formation does not contain any recycled Upper Vendian white micas. This concurs with the suggestion that Proterozoic sandstones and their potential source areas were covered by an Upper Devonian carbonate

platform at the same time as the Zilair Formation was deposited, as indicated by the widely exposed Lower Palaeozoic unconformity on the Beloretzk Terrane (Puchkov, 1997). Therefore, this area cannot have been a potential source for phengites in the Zilair Formation. In addition, our data suggest that other Proterozoic metamorphic rocks, a potential source area that might have occurred in the suture zone possibly overlying rocks of the Maksyutovo Complex, were not exposed during deposition of the Zilair Formation.

The spread of ages from the four analysed samples collected from different stratigraphic and regional positions within the Zilair Formation is similar, suggesting a similar composition and source of the Zilair detritus in space and time (Willner *et al.* 2002a). Although our ages have large errors, most of the phengites of the younger age range of 342–421 Ma seem to be older than the estimated time of peak metamorphism at  $375 \pm 2$  Ma (Glodny *et al.* 2002) of the high-pressure rocks of the current lower Unit 1 in the Maksyutovo Complex. A paradox seems to occur in this situation. The absolute time span of sedimentation of the Zilair Formation (~354–376 Ma; see above) coincides well with the initial exhumation of the Maksyutovo Complex between  $375 \pm 2$  Ma and  $360 \pm 8$  Ma at moderate rates of 2–3 mm a<sup>-1</sup> (Hetzl & Romer, 2000). However, Brown, Hetzel & Scarrow (2000) and Leech & Stockli (2000) proposed residence of the presently exposed high-pressure rocks of Unit 1 at a crustal level of 20–25 km after 355 Ma, and a slowing down of exhumation rates to 0.3 mm a<sup>-1</sup> up until 315 Ma. Hence, the presently exposed high-pressure rocks cannot be the direct source of the Zilair detritus. On the other hand, detrital components such as chloritoid, glaucophane and garnet were also typically found in the Zilair detritus and match the composition of respective minerals from the lower Unit 1 of the Maksyutovo Complex (Willner *et al.* 2002a). This means that high-pressure rocks similar to those of Unit 1 were already exhumed to the surface during the deposition of the Zilair Formation. To solve this paradox, we propose that continuous exhumation of high-pressure rocks to the surface after arc–continent collision occurred over a certain period. If we take the initial moderate exhumation rates derived from the presently exposed Maksyutovo rocks into account, the peak of high-pressure metamorphism of the first high-pressure rocks at the surface should have been older than 375 Ma and should closely correspond to the Givetian time interval (387–382 Ma), when European continental crust arrived at the subduction zone (Brown *et al.* 2001). Brown, Hetzel & Scarrow (2000) proposed concomitant subduction during the exhumation process. With this setting prevailing during a certain period, a circulation with upward flow of high-pressure rocks compensated by concomitant subduction of upper crustal rocks will occur rather than a single pass process. Hence, the much younger white mica ages

of the upper Unit 2 of the Maksyutovo Complex (332–339 Ma Beane & Connelly, 2000; Schulte & Sindern, 2002) could also rather indicate later subduction during this cyclic process. Such circulation during exhumation of collisional high-pressure rocks was modelled by Willner *et al.* (2002b) and Gerya *et al.* (2002).

The three Zilair Formation muscovite grains that yielded older ages of  $446 \pm 54$ ,  $468 \pm 28$  and  $496 \pm 2$  Ma cannot be easily attributed to a particular source or to processes known in the Southern Urals at that time. However, nothing is yet known about the age distribution of white micas in the low grade Suvanyak Complex to the west of the Maksyutovo Complex, which is also a potential source area. In addition, partially reset Precambrian ages cannot be excluded as an explanation for the presence of these three older ages.

## 6. Conclusions

Our study shows that a combined characterization of the chemical composition and the age of detrital white micas can better discriminate detritus populations related to different source rocks and finally help to refine current exhumation models of high-pressure rocks. Using the *in situ* ultraviolet laser ablation Ar–Ar dating technique we were able to discriminate phengite-bearing age groups from phengite-free groups within two different detrital populations derived from uplifting high-relief areas, where high-pressure rocks were contemporaneously exhumed. Although the individual Ar–Ar age errors were large due to low gas yields obtained from the small grains, age signatures are compatible with known data from supposed source areas and corroborate suggestions from earlier detritus analyses (Willner *et al.* 2001, 2002a, 2003).

The age signatures of the white micas from the Upper Vendian and the Famennian synorogenic sediments in the Southern Urals do not overlap, showing two different source areas containing high-pressure rocks of different ages. However, a bimodal distribution of ages and chemical composition was detected in the two different detrital populations.

The detrital white micas from the Upper Vendian sandstones show (1) a younger age group of 571–609 Ma with phengitic compositions only and (2) an older age group of 645–732 Ma containing muscovite compositions only. The first is compatible with exhumation and cooling of a source area containing high-pressure rocks, from the exotic Neoproterozoic Beloretzk Terrane that was emplaced and eroded concomitant with the deposition of the sandstones. The second age group refers to muscovites of magmatic or metamorphic origin compatible with a long history of cooling and exhumation of the source area, but incompatible with any event in the underlying Riphean basin exposed to the west. It shows that only the Beloretzk Terrane was contributing detritus to the

synorogenic Upper Vendian sediments and underlines its allochthonous nature. Its emplacement marks a change from passive to active margin conditions in the Southern Urals at  $\sim 620$  Ma.

The detrital white micas from the Upper Devonian Zilair Formation show (1) an age group of 342–421 Ma containing phengites as well as muscovites and (2) a second group of 446–496 Ma containing muscovites only. While the derivation of the second group cannot be correlated with known data, the first group is compatible with derivation from a high-pressure rock source undergoing exhumation during deposition of the synorogenic Zilair sandstones. It indicates the earliest arrival of high-pressure rocks at the surface after the onset of subduction of continental crust at the site of the present Maksyutovo Complex. In addition to other detritus minerals (glaucofane, garnet with similar compositional and zoning characteristics), it further shows similarity to high-pressure rocks in the actual lower part of the Maksyutovo Complex. However, these rocks were exposed much later than the deposition of the Zilair Formation. One possible interpretation is that continent collision-related high-pressure rocks have continuously been exhumed during a circulation process over a certain period of time compensated by concomitant subduction of upper crust.

**Acknowledgements.** Financial support by the Deutsche Forschungsgemeinschaft (Wi 875-6/2) is gratefully acknowledged. Detailed reviews by T. Barry and D. Brown considerably improved the paper. This paper is also a contribution to EUROPROBE (URALIDES). Europrobe is coordinated within the International Lithosphere Program and sponsored by the European Science Foundation.

## References

- ALVAREZ MARRÓN, A., BROWN, D., PÉREZ-ESTAÚN, A., PUCHKOV, V. & GOROZHANINA, Y. 2000. Accretionary complex structure and kinematics during Paleozoic arc-continent collision in the Southern Urals. *Tectonophysics* **325**, 175–91.
- BEANE, R. J. & CONNELLY, J. N. 2000.  $^{40}\text{Ar}/^{39}\text{Ar}$ , U–Pb and Sm–Nd constraints on the timing of metamorphic events in the Maksyutov Complex, southern Ural Mountains. *Journal of the Geological Society, London* **157**, 811–22.
- BEANE, R. J., LIU, J. G., COLEMAN, R. G. & LEECH, M. L. 1995. Petrology and retrograde P–T path for eclogites of the Maksyutov Complex, southern Ural mountains, Russia. *Island Arc* **4**, 254–66.
- BROWN, D., ALVAREZ-MARRÓN, J., PÉREZ-ESTAÚN, A., GOROZHANINA, Y., BARYSHEV, V. & PUCHKOV, V. N. 1997. Geometric and kinematic evolution of the foreland thrust and fold belt in the southern Urals. *Tectonics* **16**, 551–62.
- BROWN, D., ALVAREZ-MARRÓN, J., PÉREZ-ESTAÚN, A., PUCHKOV, V. N., GOROZHANINA, Y. & AYARZA, P. 2001. Structure and evolution of the Magnitogorsk forearc basin: Identifying upper crustal processes during arc-continent collision in the southern Urals. *Tectonics* **20**, 364–75.

- BROWN, D., HETZEL, R. & SCARROW, J. H. 2000. Tracking arc-continent collision subduction zone processes from high-pressure rocks in the southern Urals. *Journal of the Geological Society, London* **157**, 901–4.
- BROWN, D., JUHLIN, C., ALVAREZ-MARRÓN, J., PÉREZ-ESTAÚN, A. & OSLIANSKI, A. 1998. Crustal-scale structure and evolution of an arc-continent collision zone in the southern Urals, Russia. *Tectonics* **17**, 158–71.
- CLAUER, N. 1981. Strontium and Argon isotopes in naturally weathered biotites, muscovites and feldspars. *Chemical Geology* **31**, 325–34.
- COPELAND, P. & HARRISON, T. M. 1990. Episodic rapid uplift in the Himalaya revealed by  $^{40}\text{Ar}/^{39}\text{Ar}$  analysis of detrital K-feldspar and muscovite, Bengal fan. *Geology* **18**, 354–7.
- GERYA, T. V., STÖCKHERT, B. & PERCHUK, A. L. 2002. Exhumation of high-pressure metamorphic rocks in a subduction channel: A numerical simulation. *Tectonics* **21**, 6-1–6-19.
- GIESE, U., GLASMACHER, U. A., KOZLOV, V. I., MATENAAR, I., PUCHKOV, V. N., STROINK, L., BAUER, W., LADAGE, S. & WALTER, R. 1999. Structural framework of the Bashkirian anticlinorium, SW Urals. *Geologische Rundschau* **87**, 526–44.
- GLASMACHER, U. A., BAUER, W., GIESE, U., REYNOLDS, P., KOBER, B., PUCHKOV, V. N., STROINK, L., ALEKSEYEV, A. & WILLNER, A. P. 2001. The metamorphic complex of Beloretzk, SW Urals, Russia – a terrane with a polyphase Meso- to Neoproterozoic thermo-dynamic evolution. *Precambrian Research* **110**, 185–213.
- GLASMACHER, U. A., REYNOLDS, P., ALEKSEYEV, A. A., PUCHKOV, V. N., TAYLOR, K., GOROZHANIN, V. & WALTER, R. 1999.  $^{40}\text{Ar}/^{39}\text{Ar}$  Thermochronology west of the Main Uralian fault, southern Urals, Russia. *Geologische Rundschau* **87**, 515–25.
- GLODNY, J., BINGEN, B., AUSTRHEIM, H., MOLINA, J. F. & RUSIN, A. 2002. Precise eclogitization ages deduced from Rb/Sr mineral systematics: The Maksyutov complex, Southern Urals, Russia. *Geochimica et Cosmochimica Acta* **66**, 1221–35.
- HAMES, W. E. & BOWRING, S. A. 1994. An empirical evaluation of the argon diffusion geometry in muscovite. *Earth and Planetary Science Letters* **124**, 161–9.
- HESS, J. C. & LIPPOLT, H. J. 1986. Kinetics of Ar isotopes during neutron irradiation:  $^{39}\text{Ar}$  loss from minerals as a source of error in  $^{40}\text{Ar}/^{39}\text{Ar}$  dating. *Chemical Geology (Isotope Geoscience Section)* **59**, 223–36.
- HETZEL, R. 1999. Geology and geodynamic evolution of the high-P/low-T Maksyutov Complex, southern Urals, Russia. *Geologische Rundschau* **87**, 577–88.
- HETZEL, R., ECHTLER, H. P., SEIFERT, W., SCHULTE, B. A. & IVANOV, K. S. 1998. Subduction- and exhumation-related fabrics in the Paleozoic high pressure/low-temperature Maksyutov complex, Antingan area, southern Urals, Russia. *Geological Society of America Bulletin* **110**, 916–30.
- HETZEL, R. & ROMER, R. L. 2000. A moderate exhumation rate for the high-pressure Maksyutov Complex, southern Urals, Russia. *Geological Journal* **35**, 327–44.
- KELLEY, S. P. & BLUCK, B. J. 1992. Laser  $^{40}\text{Ar}/^{39}\text{Ar}$  ages for individual detrital muscovites in the Southern Uplands of Scotland, U.K. *Chemical Geology (Isotope Geoscience Section)* **101**, 143–56.
- LEECH, M. L. & STOCKLI, D. F. 2000. Exhumation history of the ultrahigh-pressure Maksyutov Complex, southern Urals mountains, from new apatite fission-track data. *Tectonics* **19**, 153–67.
- LENNYKH, V. I., VALIZER, P. M., BEANE, R., LEECH, M. & ERNST, W. G. 1995. Petrotectonic evolution of the Maksyutov Complex, southern Urals, Russia: implications for ultra-high-pressure metamorphism. *International Geology Review* **37**, 584–600.
- LO, C-H. & ONSTOTT, T. C. 1989.  $^{39}\text{Ar}$  recoil artifacts in chloritized biotite. *Geochimica et Cosmochimica Acta* **53**, 2697–711.
- MASLOV, A. V., ERDTMANN, B.-D., IVANOV, K. S. & KRUPENIN, M. T. 1997. The main tectonic events, depositional history, and the paleogeography of the southern Urals during the Riphean-early Paleozoic. *Tectonophysics* **276**, 313–35.
- MASSONNE, H.-J. 1995. Experimental and petrogenetic study of UHPM. In *Ultrahigh pressure metamorphism* (eds R. G. Coleman and X. Wang), pp. 33–95. Cambridge: Cambridge University Press.
- MASSONNE, H.-J. & SCHREYER, W. 1987. Phengite geobarometry based on the limiting assemblage with K-feldspar, phlogopite and quartz. *Contributions to Mineralogy and Petrology* **96**, 212–24.
- MATENAAR, I., GLASMACHER, U. A., PICKEL, W., GIESE, U., PAZUKHIN, V. N., KOZLOV, V. I., PUCHKOV, V. N., STROINK, L. & WALTER, R. 1999. Incipient metamorphism between Ufa and Beloretzk, western fold-and-thrust belt, southern Urals, Russia. *Geologische Rundschau* **87**, 545–60.
- MATTE, P., MALUSKI, H., CABY, R., NICHOLAS, A., KEPEZHINSKAS, P. & SOBOLEV, S. 1993. Geodynamic model and  $^{39}\text{Ar}/^{40}\text{Ar}$  dating for the generation and emplacement of the high pressure metamorphic rocks in the SW Urals. *Comptes Rendus de l'Académie des Sciences Paris* **317**, 1667–74.
- MCDOWELL, D. S. & ELDERS, W. A. 1980. Authigenic layer silicate minerals in borehole Elmore 1, Salton Sea Geothermal Field, California, USA. *Contributions to Mineralogy and Petrology* **74**, 293–310.
- ODIN, G.-S. & ODIN, CH. (eds) 1990. *Geochronologique*. Bureau des Recherches Géologiques et Minières, Société Géologique de France.
- PAZUKHIN, V. N., PUCHKOV, V. N. & BARYSHEV, V. N. 1996. New data on the stratigraphy of the Zilair series (Southern Urals). *Yearbook 1995 Institute of Geology, Ufimian Science Centre, Russian Academy of Science Ufa*, 34–41 [in Russian].
- PUCHKOV, V. N. 1997. Structure and geodynamics of the Uralian orogen. In *Orogeny Through Time* (eds J.-P. Burg and M. Ford), pp. 201–36. Geological Society of London, Special Publication no. 121.
- PUCHKOV, V. N. 2000. *Paleogeodynamics of the Southern and Middle Urals*. Ufa (Russia): Dauria, 146 pp. [in Russian].
- SCHULTE, B. A. & BLÜMEL, P. 1999. Metamorphic evolution of eclogite and associated garnet–mica schist in the high-pressure metamorphic Maksyutov complex, Ural, Russia. *Geologische Rundschau* **87**, 561–76.
- SCHULTE, B. A. & SINDERN, S. 2002. K-rich fluid metasomatism at high-pressure metamorphic conditions: lawsonite decomposition in rodingitized ultramafite of the Maksyutov Complex, Southern Urals (Russia). *Journal of Metamorphic Geology* **20**, 529–41.
- SHATSKY, V. S., JAGOUTZ, E. & KOZ'MENKO, O. A. 1997. Sm–Nd dating of the high-pressure metamorphism

- of the Maksyutov Complex, southern Urals. *Doklady (Earth Sciences Section)* **353**, 285–8.
- STEIGER, R. J. & JÄGER, E. 1977. Subcommission on geochronology: Convention on the use of decay constants in geo- and cosmochronology. *Earth and Planetary Science Letters* **36**, 359–62.
- STUART, F. M. 2002. The exhumation history of orogenic belts from  $^{40}\text{Ar}/^{39}\text{Ar}$  ages of detrital micas. *Mineralogical Magazine* **66**, 121–35.
- TUCKER, R. D., BRADLEY, D. C., VER STRAETEN, C. A., HARRIS, A. G., EBERT, J. R. & MCCUTCHEON, S. R. 1998. New U–Pb zircon ages and the duration and division of Devonian time. *Earth and Planetary Science Letters* **158**, 175–86.
- WILLNER, A. P., ERMOLAEVA, T., STROINK, L., GIESE, U., GLASMACHER, U. A., PUCHKOV, V. M., KOZLOV, V. I. & WALTER, R. 2001. Contrasting provenance signals in Riphean and Vendian sandstones in the SW Urals (Russia): constraints for a change from passive to active continental margin conditions in the Late Precambrian. *Precambrian Research* **110**, 215–39.
- WILLNER, A. P., ERMOLAEVA, T., GOROZHANINA, Y. N., PUCHKOV, V. N., ARZHAVITINA, M., PAZUKHIN, V. N., KRAMM, U. & WALTER, R. 2002a. Surface signals of an arc–continent collision: the detritus of the Upper Devonian Zilair Formation in the Southern Urals/Russia. In *Mountain Building in the Uralides: Pangea to the Present* (eds D. Brown, C. Juhlin and V. N. Puchkov), pp. 183–209. American Geophysical Union Monograph no. 132.
- WILLNER, A. P., SEBAZUNGU, E., GERYA, T., MARESCH, W. V. & KROHE, A. 2002b. Numerical modeling of PT-paths related to rapid exhumation of high-pressure rocks from the crustal root in the Variscan Erzgebirge Dome, Saxony/Germany. *Journal of Geodynamics* **32**, 281–314.
- WILLNER, A. P., SINDERN, S., METZGER, R., ERMOLAEVA, T., KRAMM, U., PUCHKOV, V. N. & KRONZ, A. 2003. Typology and single grain U/Pb systematics of detrital zircon from Neoproterozoic sandstones in the SW Urals (Russia): early time markers at the eastern margin of Baltica. *Precambrian Research* **124**, 1–20.

### Appendix. Sample localities

U21 – sandstone of the Upper Vendian Zigan Formation; outcrop along the Tolparovo–Mendim road, 3 km W of the bridge across the Takati River.

Z8 – sandstone of the Lower Zilair Formation (directly above the Mukas Cherts; Magnitogorsk zone); quarry N of Mukasevo.

Z15 – sandstone of the Middle Zilair Formation (Astashian Member; Zilair zone); outcrop along the Zilair-Kugartschi road in the village of Verchnjaja Kazarma.

Z19 – sandstone of the Middle Zilair Formation (Upper part of the Avashlinian Member; Zilair Zone); outcrop along the Zilair–Kugartschi road at the bridge across the Ergaschi River.

Z28 – sandstone of the Lower Zilair Formation (Yaumbayevian Member; Main Uralian Fault Zone); outcrop on the eastern bank of the Turatka River 2 km N of the Ulgan–Kurgan gorge and S of Iljatschevo.